

**Microprobe Dating of Monazite in Relation to
Porphyroblast Growth and Thermodynamic Modelling
P-T paths for Rocks Affected by Prolonged Orogenesis**

VOLUME I

Thesis submitted by
Peter W. Welch (M.S. Virginia Tech)
in April 2003

For the degree of Doctor of Philosophy
in the School of Earth Sciences
James Cook University
Townsville, Australia

STATEMENT OF ACCESS

I, the undersigned author of this thesis, understand that James Cook University will make this thesis available for use within the university library as well as by microfilm and other means and allow access to other users in approved libraries.

All users consulting this thesis will have to sign the following statement:

In consulting this thesis, I agree not to copy closely or paraphrase it in whole or in part without the written consent of the author; and to make proper public written acknowledgement for any assistance that I have obtained from it.

Beyond this, I do not wish to place any restrictions on access to this thesis.

Peter W. Welch

April 2003

ABSTRACT. Pressure-Temperature-time-deformation paths were modelled using microstructural, petrologic, geochronologic data for multiply deformed Acadian metamorphic rocks currently exposed within and mantling the Chester and Athens Domes in southeastern Vermont, USA. Estimates of pressure, temperature and time were obtained for samples where the relative timing of distinct periods of garnet growth has been previously established through detailed microstructural analysis of foliation intersection axes (FIAs) of inclusion trails in garnet porphyroblast.

Compositional mapping and *in-situ* microprobe analyses of monazite grains reveal that monazite growth was the result a series of reactions or growth events. Numerous monazite grains preserve complex compositional zoning patterns that cannot be easily explained by a single monazite growth event. Electron microprobe point analyses of U, Th, Pb and Y were used to determine the ages of monazite grains or distinct compositional domains within monazite grains. U-Th-Pb age distributions show monazite growth and subsequent metamorphism occurred over a period at least 80 m.y from 430 Ma to 350 Ma. A single sample was found to contain distinct populations when monazites were grouped by microstructural affinities. A single sample yielded ages of 424 ± 2.4 Ma, 405 ± 6.0 Ma, 386 ± 6.0 Ma, 366 ± 3.8 for monazite populations analysed in the cores, medians, and rims of garnet porphyroblasts and matrix respectively. Weighted averages calculated for monazite populations, which lie within the included/overgrown foliations for all of the samples clustered around 425 Ma, 405, Ma, 387 Ma, 377, Ma and 365 Ma and 350 Ma. These age distributions are taken to represent a best estimate of the timing of deformation and accompanying mineral growth for southeastern Vermont.

P-T pseudosections were utilised to map mineral reactions for samples that contain garnet porphyroblasts with inclusion mineralogies that reveal partial mineral assemblages prior to garnet growth. Pseudosections were modelled in the system MnKFMASH for high-Al pelites and MnNCKFMASH for low-Al pelites and calc-pelites. Thermobarometric calculations were compared with P-T pseudosections to construct P-T paths consistent with observed mineral reactions. P-T estimates for garnet cores are consistent with the position of garnet-in reactions on MnKFMASH pseudosections and are generally 25-50°C above the garnet-in reaction on the MnNCKFMASH pseudosections. P-T estimates for garnet cores reveal that garnet growth commenced at \square 525°C and moderate pressure (4-9 kbars) and proceeded along an up-pressure path reaching peak pressures between 13-14 kbars at 600-625°C. Monazite inclusions in garnet porphyroblasts bracket the timing of the onset of garnet growth between 425 Ma and 405 Ma. Peak pressure, which is estimated to have occurred at \square 600°C, was likely reached by 385 Ma. Peak temperatures of \square 650°C are recorded between 11-12 kbars, which was followed by decompression and cooling. Decompression occurred between 380 and 350 Ma with very little heating indicating that initial uplift and subsequently exhumation was rapid. Monazite ages from garnet rims and matrix mark the end deformation and mineral growth at 350 Ma.

Previous tectonic models for Acadian orogenesis for the region have suggested that deformation and accompanying metamorphism was a two-stage process. Crustal thickening was thought to be the result of nappe style thrusting followed by regional scale doming. The integration of microstructural studies and *in-situ* monazite dating along with a detailed evaluation of the thermobarometric history reveals a more complex deformation and metamorphic history. The peak pressures and relatively low geothermal gradients associated with the early part of the P-T path are more consistent with subduction related tectonism than nappe style thrusting. Inclusion trails in garnet porphyroblasts also reveal that numerous near orthogonal foliations formed during

garnet growth that cannot be easily explained by nappe and dome stage deformations. In the proposed model, foliation development and subsequent mineral growth occurs in response to crustal thickening related to continental subduction. This resulted in a greatly over-thickened crust that was unstable and underwent rapid uplift and exhumation with little heating. Monazite ages that have been linked directly with microstructures and mineral growth reveal that Acadian Orogenesis may have begun as early as the earliest Silurian and continued through to the Carboniferous.

ACKNOWLEDGMENTS

First and foremost, I would like to acknowledge Professor Tim Bell for all of his support and tireless efforts. Tim presented me with the opportunity to explore my own ideas under his tutelage in such a way that I feel I have benefited immensely. I enjoyed working with Tim and I can only hope that it has been a fruitful experience for us both. I would also like to acknowledge Dr. Ken Hickey for his support at the onset of my Ph.D.; his presence at James Cook University has been sorely missed. Ken Hickey and Tim Bell are also acknowledged for providing the samples and vast thin-section collection used for this research. I am indebted to all of the people who have passed through SAMRI during my tenure, especially Cameron Huddleston-Holmes, Nick Timms, Andrew Ham and Tom Evans. Tom has contributed significantly to my project by expertly working through some of our THERMOCALC problems where I did not have the ability or patience. The Faculty and staff of School of Earth Sciences are also recognised for their support and assistance.

Funding for my Ph.D. was provided by an Overseas Postgraduate Research Scholarship and a School of Earth Sciences Scholarship. Financial support used to cover the cost of research was partly provided by an Australian Research Council grant given to Tim Bell as well as by two Doctoral Merit Research Grants provided by James Cook University. The final stages of writing were also supported by an additional scholarship provided by James Cook University. The School of Earth Sciences is also acknowledged for financial support used to cover basic research costs.

The Advanced Analytical Center at James Cook University provided a superb facility for data collection as well as other technical support. Special thanks go to Dr. Kevin Blake for all of his support with Microprobe analysis. He was able to push the JEOL-840 microprobe at JCU to produce results that neither one of thought possible. Monazite analyses were collected at the Dept. of Geological Sciences at the University of Massachusetts with the assistance of Mike Williams and Mike Jercinovic. They are both acknowledged for continued technical support and feedback on ideas and problems related to monazite analysis and data interpretation. I would like also like to thank Dr. Ian Fitzsimon at Curtin University for collecting the SHRIMP data for me. Dr. Hideyuki Takahashi was kind enough to give me the high quality images that he collected at the JEOL research lab in Japan.

I also owe tremendous thanks to my family. They have always supported and encouraged me in every endeavor I have undertaken. Living on opposite ends of the world would have been difficult without the endless support of my mother and father, Kevin, Sue, Kathy, and Mimi. I should also acknowledge/blame my two sisters, Sue and Kathy, both of whom are accomplished geoscientist for pointing me in this direction many years ago. And of course, I am most grateful for the support of my loving partner Rhonda. She has helped me in ways too numerous to express through this experience while she was working on a dissertation herself. I would not have had it any other way!

TABLE OF CONTENTS

Thesis Abstract	ii
Acknowledgements	iv
List of Figures and Tables	viii
Preface	xii

**Chapter 1 - Episodic Deformation and Metamorphism in Southeastern Vermont:
New Age Constraints from Electron Microprobe and SHRIMP Analysis of
Monazite Inclusions in Garnet.**

ABSTRACT	2
INTRODUCTION	2
GEOLOGIC SETTING AND PREVIOUS STUDIES	4
BACKGROUND	6
METHODS	7
Petrography	7
Monazite compositional mapping	10
Major and trace element analyses	11
SHRIMP analysis	12
RESULTS and INTERPRETATIONS	13
Monazite chemistry and compositional zoning	13
Microprobe age determination and uncertainties	15
Microprobe and SHRIMP monazite ages	16
Total microprobe dataset	19
DISCUSSION and CONCLUSIONS	20
Monazite growth history in relation to metamorphism	20
Age distribution	22
Age of orogenesis (Taconian vs. Acadian)	23
REFERENCES	26

**Chapter 2 - Prolonged Acadian Orogenesis: Revelations from Foliation
Intersection Axis (FIA) controlled Monazite Dating of Foliations in Porphyroblasts
and Matrix.**

ABSTRACT	31
INTRODUCTION	31
GEOLOGIC SETTING	32
SAMPLES DATED	34
AGES	36
Age determination	36
Foliations, FIA sets and their monazite ages	38
The combined age data set	39
INTERPRETATION	39
Foliation development and preservation as inclusion trails	39
Monazite behaviour during foliation development	40
Monazite microstructural relationships	41
Interpretation of the ages obtained from each sample	42
Significance of monazite ages and episodic porphyroblast	

growth reactions	44
Foliation ages versus porphyroblast ages	45
Correlation of ages with FIA trends	46
FIA versus matrix ages	46
DISCUSSION	47
The heterogeneity of deformation and FIA development	47
Confirmation of the episodic nature of metamorphism	48
Significance of episodic growth of porphyroblasts	49
The age of the Acadian	49
Acadian versus Taconic Orogenesis	50
Continuity of plate motion versus few matrix deformation events	50
REFERENCES	52

Chapter 3 – Linking Deformation and Metamorphism: Pressure-Temperature-time-deformation Paths through Quantitative Microstructural Analysis and Pseudosections.

ABSTRACT	58
INTRODUCTION	59
REGIONAL GEOLOGIC SETTING	61
Metamorphic and structural setting of SE Vermont	62
Samples	64
METHODS	65
FIAS and microstructures	65
Compositional mapping	67
Mineral and bulk compositions	68
MONAZITE AGES	69
INTERPRETATION	70
Thermobarometry	70
Phase equilibria and P-T pseudosections	72
Integration of mineral assemblages, pseudosections, FIA development and thermobarometry.	74
DISCUSSION	77
Microstructures and mineral zoning	77
The anomalous Mn content in garnet	79
Tectonic significance of the Mn excursion	80
Integration of metamorphic and structural approaches	80
REFERENCES	84

Chapter 4 – Pressure-Temperature Paths and the Relationship between Garnet Producing Reactions, Microstructural Truncations and Mineral Zoning.

ABSTRACT	89
INTRODUCTION	90
GEOLOGIC SETTING	91
SAMPLES and PETROGRAPHY	92
METHODS and RESULTS	94
Mineral compositions and compositional maps	94

Bulk compositions and chemical systems	96
Pseudosections	97
Thermobarometry	98
INTERPRETATIONS	100
General phase relationships and pseudosections	100
Garnet producing reactions	102
P-T evolutions	102
P-T path in relation to the pseudosections	103
Mineral zoning and truncations	104
DISCUSSION	106
Equilibrium and reaction overstepping	106
Equilibrium and deformation	107
Metamorphic and microstructural significance	108
Regional and tectonic significance	109
REFERENCES	111

LIST OF FIGURES AND TABLES- VOLUME II

Preface

- Figure 1.** Geologic maps of the Chester and Athens Domes and the Spring Hill Synform with sample locations used in this study along with generalised geologic map of New England. iv
- Figure 2.** Schematic diagram illustrating a FIA on vertical thin-sections. v

Chapter 1 - Episodic Deformation and Metamorphism in Southeastern Vermont: New Age Constraints from Electron Microprobe and SHRIMP Analysis of Monazite Inclusions in Garnet

- Figure 1.** Geology of Chester and Athens Domes and Sample Locations. 2
- Figure 2.** V436A monazite photomicrograph. 3
- Figure 3.** BSE images of sample V634A. 4
- Figure 4.** BSE images of sample V436A. 5
- Figure 5.** Photomicrograph and BSE images for sample V436B 6
- Figure 6.** BSE images of sample V653. 7
- Figure 7.** BSE images of sample V240. 8
- Figure 8.** BSE images of monazite grains showing SHRIMP pits. 9
- Figure 9.** X-ray compositional maps for monazite grain V634A-Mz4. 10
- Figure 10.** X-ray compositional maps for monazite grains from sample V436A. 11
- Figure 11.** X-ray compositional maps for monazite grains from sample V653. 12
- Figure 12.** X-ray compositional maps for monazite grain V436B-Mz1. 12
- Figure 13.** X-ray compositional maps for monazite grains from sample V240. 13
- Figure 14.** X-ray compositional maps for monazite grain V436A-Mz12 14
- Table 1.** Monazite major element analyses. 15
- Table 2.** Representative monazite trace element analyses. 16
- Table 3.** SHRIMP analyses for sample V240 and V634A. 17
- Table 4.** Electron microprobe ages list by sample. 18
- Figure 15.** Probability curves for 5 samples dated. 21
- Figure 16.** Concordia plots for SHRIMP analyses. 22
- Figure 17.** Total probability curves of age distributions. 23

Chapter 2 - Prolonged Acadian Orogenesis: Revelations from Foliation Intersection Axis (FIA) controlled Monazite Dating of Foliations in Porphyroblasts and Matrix.

- Figure 1.** Geologic map of Chester and Athens Domes. 25
- Figure 2.** Geologic map of Spring Hill Synform with sample Locations. 26
- Figure 3.** Spring Hill Synform with FIA trends. 27
- Figure 4.** Rose diagram of FIA sets. 28
- Figure 5.** V634A photomicrograph of garnet porphyroblast with line diagram. 29
- Figure 5c.** V634A garnet X-ray compositional maps. 30
- Figure 6.** V634A BSEs showing monazite locations. 31
- Figure 7.** V436A photomicrograph of garnet porphyroblast with line diagram. 32
- Figure 7c.** V436A garnet X-ray compositional maps. 33
- Figure 8.** V436A BSEs showing monazite locations. 34

Figure 9. V436B photomicrograph of garnet porphyroblast with line diagram.	35
Figure 9c. V436B garnet X-ray compositional maps.	36
Figure 10. V436B BSEs showing monazite locations.	37
Figure 11. V653 photomicrograph of garnet porphyroblast with line diagram.	38
Figure 11c. V653 garnet X-ray compositional maps.	39
Figure 12. V653 BSEs showing monazite locations.	40
Figure 13. X-ray compositional maps of monazite grains from V436A.	41
Table 1. Trace element analyses and ages for single monazite grain.	42
Table 2. Monazite ages listed by sample	43
Figure 14. Probability curves of age distribution for each sample.	46
Figure 15. Total probability curves.	47
Figure 16. Sketch of crenulation cleavage development.	49
Figure 17. Sketch of growth history for V634A.	51

Chapter 3 – Linking Deformation and Metamorphism: Pressure-Temperature-time-deformation Paths through Quantitative Microstructural Analysis and Pseudosections.

Figure 1. Geologic of Chester and Athens Domes with sample locations.	53
Figure 2. Generalized metamorphic map of southeastern Vermont.	54
Figure 3. Geology of Chester and Athens Domes with FIA trends.	55
Figure 4. V634A photomicrograph of garnet porphyroblast with line diagram.	57
Figure 4. V634A photomicrographs of inclusion trails.	58
Figure 5. V240 photomicrograph of garnet porphyroblast with line diagram.	60
Figure 5. V240 photomicrographs of inclusion trails and inclusion mineralogy.	61
Figure 5. V240 photomicrograph of staurolite porphyroblast.	62
Figure 6. V436B photomicrograph of garnet porphyroblast with line diagram.	63
Figure 7. V634A garnet X-ray compositional maps.	64
Figure 8. V240 garnet X-ray compositional maps.	65
Figure 9. X-ray compositional maps garnet core/rim interface.	66
Figure 10. V436B garnet X-ray compositional maps.	67
Table 1. Whole rock XRF results.	68
Table 2. V634A representative microprobe data.	69
Table 3. V240 representative microprobe data.	70
Figure 11. Probability curves of microprobe ages.	72
Table 4. Summary of thermobarometric results.	73
Figure 12. KFMASH and MnKFMASH petrogenetic grids.	75
Figure 13. V634A P-T pseudosections with P-T path.	76
Figure 14. V240 P-T pseudosections with P-T path.	77
Figure 15. V436B P-T pseudosections.	78
Figure 16. Photomicrographs of chloritoid schist and chloritoid inclusions.	79
Figure 17. Summary of P-T-deformation evolution.	80

Chapter 4 – Pressure-Temperature Paths and the Relationship between Garnet Producing Reactions, Microstructural Truncations and Mineral Zoning.

Figure 1. Spring Hill Geology with sample locations.	82
Figure 2. V436B photomicrograph of garnet with line drawing.	83
Figure 3. V436A photomicrograph of garnet with line drawing.	84
Figure 4. V261A photomicrograph of garnet with line drawing.	85

Figure 5. V257 photomicrograph of garnet with line drawing.	86
Figure 6. V436B garnet X-ray compositional maps.	87
Figure 7. V436A garnet X-ray compositional maps.	88
Figure 8. V261A garnet X-ray compositional maps.	89
Figure 9. V257 garnet X-ray compositional maps.	90
Table 1. Representative microprobe data for V436B.	91
Table 2. Representative microprobe data for V436A.	92
Table 3. Representative microprobe data for V261A.	93
Table 4. Representative microprobe data for V257.	95
Table 5. Whole rock XRF results used for pseudosection calculations.	97
Figure 10. AFM projection of XRF results.	98
Figure 11. P-T pseudosections for low-Al pelites.	100
Figure 12. P-T pseudosections for calc-pelites.	102
Table 6. Summary of thermobarometric results.	103
Figure 13. Interpreted P-T paths.	105
Figure 14. Summary of results for V261A.	107
Figure 15. Summary of results for V436B.	109
Figure 16. X-ray compositional maps and line drawing for 3 porphyroblasts.	110

APPENDIX

Appendix 1. Microprobe set-up for monazite analysis.	112
Appendix 2. Monazite trace element results.	113
Appendix 3. Microprobe data for V240 and V634.	120
Appendix 4. MnKFMASH datafile for THERMOCALC.	130
Appendix 5. Microprobe data for V261A, V257, V436B, V436A, V653.	137
Appendix 6. MnNCKFMASH datafile for THERMOCALC.	150
Appendix 7. JCU specimen numbers.	158

STATEMENT OF SOURCES

Declaration

I declare that this thesis is my own work and has not been submitted in any form for another degree or diploma at any university or other institute of tertiary education. Information derived from the published or unpublished work of others has been acknowledged in the text and a list of references is given

Peter W. Welch

April 2003

PREFACE

The geology in the area around the Chester and Athens Domes (see Fig. 1) in southern Vermont U.S.A. has been the center of numerous important studies in metamorphic petrology and microstructural geology. Much of our understanding of the mineral reactions that occur in pelitic rocks stemmed from early work in the area (e.g. Thompson and others 1977). This area also provided the source material for detailed studies of curved inclusion trails in garnet by Rosenfeld (1970) that led to the development of further ideas on the relationship between deformation and mineral growth. In Rosenfeld's model, curved inclusion trails provided evidence for syn-deformational garnet growth as porphyroblasts rotate as they grow. These ideas were challenged by Bell (1985), who proposed that porphyroblasts with curved inclusion trails result from grains overgrowing subsequent sets of foliations with new orientations. This reinterpretation has led to a scientific debate on the nature of curved inclusion trails that continues today. Microstructural work in the area by Bell and co-workers has led to further models for non-rotational porphyroblast growth and a more complex history for the region (e.g. Bell and others 1998).

Microstructural investigations conducted by Bell have led to a model of porphyroblast growth linked to deformation partitioning in which four distinct periods of garnet growth have been identified. These episodes of garnet growth are recognised as having distinct orientations in the axis of curvature of inclusion trails, which are referred to as **foliation intersection axis** or **FIA**. The technique for the measurement of FIAs is discussed briefly here. FIA measurements are made relative to both geographic coordinates and a line perpendicular to the earth's surface. The measurement is thus independent of assumptions, inferences, or interpretations about the timing of the inclusion trails relative to any other structures present in the rock and whether or not the porphyroblast has rotated. A FIA is recorded for a sample by locating the asymmetry switch of inclusion trails using vertical thin sections with different strikes from each sample, as shown in figure 2. A minimum of 8 vertical thin sections are required to measure a FIA trend within a 10° range, with one thin-section cut every 30° around the compass and two cut 10° apart between the sections where the asymmetry of the inclusion trails flip. There is a very significant microstructural advantage in cutting sections this way because the inclusion trails contained in many porphyroblasts can be observed from a large range of orientations, providing a much better record of the complete inclusion trail geometry than available from cutting just 1 or 2 thin sections. This presents an obvious advantage for petrologic studies, as a large number of thin-section are available for petrographic observation and corresponding thin-section blocks for preparation of polished thin-sections. In total, T.H. Bell and K. Hickey collected and prepared some 400 samples and over 2000 thin-sections for microstructural work.

The quantitative FIA measurements described in this thesis are largely the work of T.H. Bell, though microstructural observations were carried out on all of the samples described herein by the author. Some of the FIA measurements described herein were first presented in Bell and others (1998) but most have been re-examined as part of this study. The research in this thesis was developed utilizing the large sample and thin-section collection that was developed for earlier microstructural work carried out by T.H. Bell and K. Hickey. Figure 1 shows the locations for all of the samples that were utilized in this study.

The presence of 4 distinct periods of garnet growth that have been linked to a single Orogenic (Acadian) event led to the questions that have been addressed in this

thesis. The garnet growth events have been determined through geometric analysis of inclusion trails alone. This data was used to develop a model of relative timing of mineral growth. If these growth events are distinct in time and position in the crust during orogenesis then there should be some signature of this preserved in the mineral chemistry and isotopic clocks. This thesis attempts address fundamental questions on the timing and nature of metamorphic mineral growth in relation to the deformational history preserved by inclusion trails and FIAs.

The first aspect of this research deals with establishing a framework of absolute time that can be correlated with the relative timing established by FIA data. The primary technique that was chosen was U-Th-Pb dating utilising the electron microprobe. This method was chosen specifically because it provides the best opportunities to collect the analyses in-situ on standard polished thin-sections. This has the obvious advantage of linking the data directly to petrographic observation that are vital to this type of research. This method also has the added advantage of having the smallest analytical volume of all of the in-situ methods (SIMS, LA-ICPMS, SHRIMP) as well as being non-destructive. Questions surrounding the accuracy and precision of this method remain a concern. Montel and others (1996) report estimated errors of 20-30 m.y. for Palaeozoic rocks. However, it was hoped that problems surrounding the analytical uncertainties would be overcome, at least in part, by removing some of the geologic uncertainty by linking ages to individual microstructures. The first two chapters of the thesis focus on monazite geochronology. The first chapter is meant to cover the methods, results of monazite analysis, and age determination and the second focuses more on integrating this data with the voluminous microstructural data.

The second major part of the research is centred around linking the microstructural observations with petrologic models. Porphyroblasts from this region nearly always contain curved inclusion trails with many samples containing spectacular “spiralling” trails. Closer examination of these trails reveals that spiral trails are more commonly consist of sets of near orthogonal trails. Regardless of the interpretation for how these trails formed, they suggest a complex growth history for the porphyroblast that trap them. Garnet compositional maps, detailed thermobarometric studies, and P-T pseudosections were used to get a better understanding of the mineral reactions taking place and how the rocks evolve through the crust. The third chapter focuses on linking thermobarometric results to FIA data for two samples that contained monazite grains that were dated. These samples both samples contain rich inclusion suites that could be linked to microstructural observations such that a reaction history could be modelled as well. The last chapter compares and contrasts a set of simple pelites (quartz, muscovite, biotite, garnet \pm staurolite schists) with spectacular inclusion trails to a set of calc-pelites (plagioclase and epidote bearing garnet schists). Calc-pelites were used, as they are excellent for thermobarometric studies. Detailed thermobarometric results from inclusion suites and full system (MnNCKFMASH) P-T pseudosections were used to model mineral growth and construct P-T paths. As a major goal of this research, it was hoped that all of this data could be used to develop robust orogenic models for the study area that are consistent with petrologic, geochronologic and structural data.

THESIS FORMAT

This thesis consists of 4 chapters, each written as stand-alone bodies of work with the intention that they will be submitted as papers for publication. The 2nd chapter has already been published in the American Journal of Science (Bell and Welch, 2002). Taken as a whole they are intended to provide a coherent thesis examining the temporal

and petrologic evolution for the study area. Additionally, each chapter attempts to further explore some of the complex processes that occur during deformation and metamorphism. The first two chapters are centered around monazite geochronology and the second two chapters focus on modelling P-T-t-deformation paths through thermobarometric and phase equilibria studies in relation to microstructure. The 2nd chapter appears in this dissertation with only minor changes to the published version. The microstructural analysis that led to the concept for the paper was the work of Bell and he also assisted with writing and drafting figures outlining microstructure.

Chapter-1 outlines the methodology behind using the electron microprobe for monazite geochronology and discusses the results of monazite chemistry and age distributions.

Chapter-2 explores the results of the microprobe ages in the context of the development of successive deformations.

Chapter-3 focuses on the use of P-T pseudosections to examine reaction histories and develop P-T-deformation path consistent with monazite ages.

Chapter-4 explores the relationship between compositional zoning and the development of complex inclusion trails in garnet porphyroblasts. P-T pseudosections are used to model mineral reaction and construct P-T paths.

Because each chapter is designed as a stand-alone piece of work, there is a certain amount of built-in redundancy to the dissertation. Each chapter contains its own set of references and figures, which results in some of the figures being repeated. The thesis is presented as two volumes. Volume I contains the text and reference lists for each chapter Volume II contains the figures and tables for each chapter as well as all of the appendix materials.

REFERENCES

Bell, T.H., 1985, Deformation partitioning and porphyroblast rotation in metamorphic rocks: a radical reinterpretation. *Journal of Metamorphic Geology*, 3 109-118.

Bell, T.H. Hickey, K.A. and Upton, J.G., 1998, Distinguishing and correlating multiple phases of metamorphism across a multiply deformed region using axis of spiral, staircase and sigmoidal inclusion trails in garnet. 16, 767-794.

Bell T.H., and Welch, P.W., 2002, Prolonged Acadian orogenesis: Revelations from foliation intersection axis (FIA) controlled monazite dating of Foliations in porphyroblasts and matrix. *American Journal of Science*, 302, 549-581.

Montel, J.M., Foret, S; Veschambre, M, Nicollet, C, Provost, A., 1996, Electron microprobe dating of monazite. *Chemical Geology*, v. 131, n. 1-4, p. 37-53

Ratliffe, N.M., 1995a, Digital bedrock geologic map of the Cavendish Quadrangle, Vermont. US Geological Open File Report, 95-203-A.

Ratliffe, N.M., 1995b, Digital bedrock geologic map of the Chester Quadrangle, Vermont. U.S. Geologic Survey Open File Report 95-576-A.

THE IMAGE ON THIS PAGE HAS BEEN REMOVED DUE TO
COPYRIGHT RESTRICTIONS

Figure 1. Geologic of the Chester and Athens Domes and Spring Hill synform with sample locations for all of the samples used in this thesis. Geology from Ratcliffe (1995 a,b) and Ratcliffe and Armstrong (1995, 1996). CD= Chester Dome, AD= Athens Dome and SH=Spring Hill synform. Generalized geologic map of new England showing Chester and Athens Domes for reference.

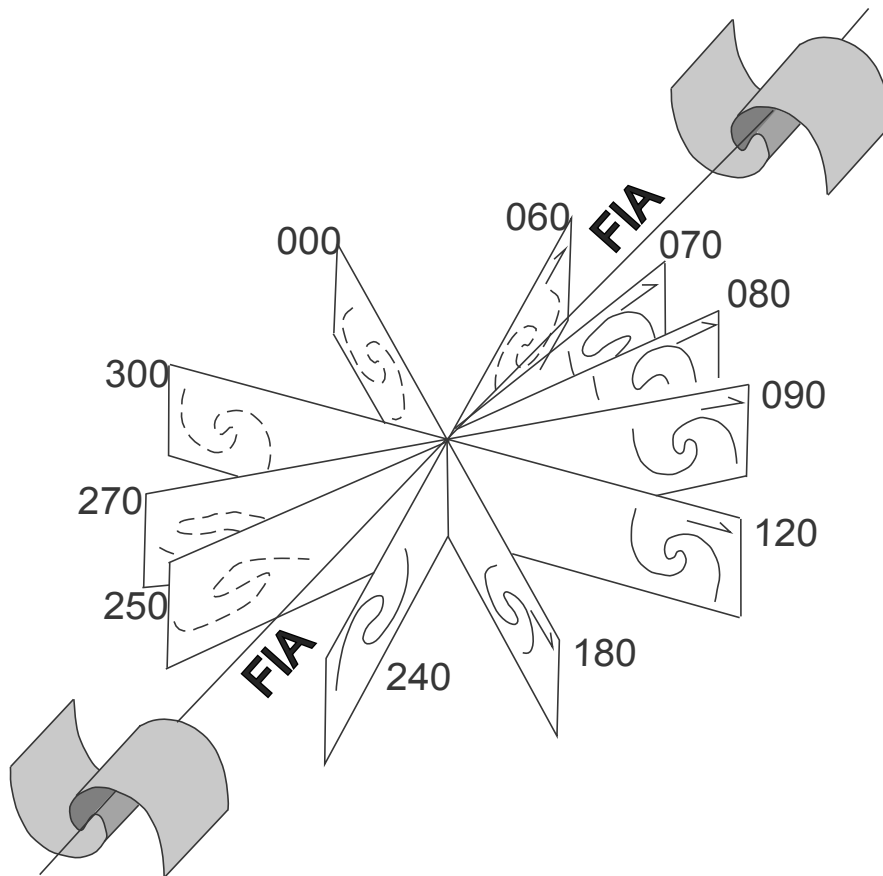


Figure 2. Schematic diagram illustrating basic methodology behind measurement of **foliation intersection axis (FIA)** of inclusion trails in garnet porphyroblasts. Curves on each thin-section represent geometry of inclusion trails in garnet porphyroblasts. True curvature is only present in thin-section perpendicular to FIA. Vertical thin-sections are prepared at 30° intervals around the compass so that a flip in the asymmetry can be identified.

Ratcliffe, N.M., and Armstrong, T.R., 1995, Preliminary bedrock geologic map of the Saxtons River 7.5°x15° Quadrangle, Windham and Windsor Counties, Vermont: U.S. Geological Survey Open-File Report 95-482.

Ratcliffe, N.M., and Armstrong, T.R., 1996, Digital bedrock geologic map of the Saxtons River 7.5°x15° Quadrangle, Windham and Windsor Counties, Vermont: U.S. Geological Survey Open-File Report 96-52-A.

Rosenfeld, J.L., 1970, Rotated garnets in metamorphic rocks. Geological Society of America Special Paper, 129.

Thompson, A.B., Lyttle, P.T., and Thompson, J.B., 1977 Mineral reactions and A-Na-K and A-F-M facies types in the Gassetts Schist, Vermont. American Journal of Science, 277, 1124-1154.

Thompson, A.B., Tracy, R.J., Lyttle, P.T., and Thompson, J.B., 1977, Prograde reaction histories deduced from compositional zonation and mineral inclusions in garnet from the Gassetts Schist, Vermont. American Journal of Science, 277, 1152-1167